Volume 17, Number 3, 2024. pp. 299-311

Jordan Journal of Physics

ARTICLE

Surface Texturing of Silicon Wafers by Two-step Ag-assisted Etching Process with New NSR Solution

Mayyadah Habeeb Hussein and **Samir Mahmmod Ahmad**

Department of Physics, College of Science, Mosul University, Mosul 41002, Iraq.

Doi: **https://doi.org/10.47011/17.3.5**

Received on: 04/08/2022; *Accepted on: 10/01/2023*

Abstract: Solar cells made of monocrystalline silicon can convert more solar energy into electrical energy if the cells can absorb greater amounts of light. Recently, it has been observed that metal-assisted catalyzed etching (MACE) is a good technology for manufacturing micro and nanostructures on silicon substrates. In this work, we use silver as a catalyst in a two-step metal-assisted etching process followed by a rebuilding nanostructure (NSR). We study the effect of changing the parameters of the second step in the MACE process (concentrations of etching solution materials, temperature, and reaction time), where black silicon was obtained with a reduced reflection of 3% without the NSR process. We tested the effect of two types of alkaline solutions in the NSR process on the surface structure of silicon. After performing an NSR operation with sodium hydroxide solution, the field emission scanning electron microscopy (FESEM) image shows a surface with upright pyramidal structures intertwined with deep cavities, and with a reflectance of 10.74%. However, after performing the NSR process with a solution of sodium silicate, the FESEM image shows a rough surface with non-overlapping pores of small cross-sections, achieving a reflectance of 8.65% within the wavelength range of 550-850nm.

Keywords: Texturing, Monocrystalline silicon, Ag-assistance chemical etching, Black silicon, Reflectance.

Introduction

Solar cells are considered one of the promising technologies in the field of renewable energy due to their potential for low-carbon energy production and cost reduction [1]. Despite expectations that their production costs had reached a minimum, they have decreased by another 20% [2]. The field of photovoltaics has witnessed significant advancements in recent years, with ongoing studies aimed at increasing the capacity of cells and reducing production costs [3]. Crystalline silicon cells dominate the solar cell market, accounting for 90% of the global photovoltaic market [4].

The dominance of silicon photovoltaic cells can be attributed to several factors: silicon is abundant, making it inexpensive and non-toxic, with its energy gap is almost suitable for the solar spectrum [4, 5]. However, one of its main disadvantages is its low photon absorption which results in lower cell efficiency [4]. Therefore, absorbance must be increased, either by using an anti-reflection coating [6, 7] or by the texturing process [8]. Texturizing the silicon surface leads to the formation of micro- or nanostructures, which alter the mechanical and electrical properties of the surface [9].

The indirect bandgap of silicon makes it difficult to transfer electrons from the valence band to the conduction band [4]. However, nanoscale silicon structures such as porous silicon [10], quantum dots [11], and nanowires [12], have a direct bandgap, facilitating easier electron movement between the valence and conduction bands.

Corresponding Author: Mayyadah Habeeb Hussein **Email**: gardenrose81522@gmail.com

The texturing process on crystalline silicon wafers can be carried out in several ways, including lithography [13], mechanical grooving [13, 14], reactive ion texturing [16], laser texturing [17], acidic texturing [18], alkaline texturing [19], and metal assistant chemical etching [20]. The efficiency of a solar cell can be increased by performing a wet chemical etching process with the help of metals, either in a single-step [21] or two-step [22] procedure. MACE, one of many fabrication techniques, has become popular as a low-cost, adaptable method for creating Si nanostructures with simple control over position, diameter, and length [22-24]. In MACE, a Si substrate is etched in an oxidant-containing HF solution using noble metal particles or membranes with pores. Si substrates covered in noble metal particles or films etch substantially more quickly than those without metal coverage. Thus, the morphology of the resultant Si nanostructures can be modified by varying the morphology of the precipitated noble metal.

The nanostructure rebuilding (NSR) process is used to change the shape of the nanostructure formed by chemical etching with the help of minerals on the silicon surface and to enhance the light absorption process [26]. Pu *et al.* reported that a one-step metal-assisted chemical etching process using Ag/Cu, followed by the NSR process, leads to the formation of uniform inverted pyramids with a reflection rate of 19.77% [27]. Chen *et al.* applied the two-step metal-assisted chemical etching process to single and multicrystalline silicon wafers, achieving reflectivity rates of 19.4% and 18.7%, respectively [28].

In this work, we textured monocrystalline silicon wafers using a two-step metal-assisted chemical etching process followed by the NSR process. We varied the main parameters of the second step in the metal-assisted etching process (concentration, temperature, and reaction time) and compared the use of sodium hydroxide with a new solution of sodium silicate in the NSR process.

Materials and Methods

This study used P-type (Nexolon) monocrystalline silicon wafers, 200 ± 20 µm thick, with an area of 6 cm^2 and resistivity of 0.5-3.0Ω.cm as substrates. To remove saw damage, the wafers were dipped in a 10% sodium hydroxide solution (KOH) for 15 min at 75°C, followed by immersion in a 10% hydrofluoric acid (HF) solution at room temperature for 2 min to remove the native oxide.

The two-step MACE process involved a first step with a solution of $AgNO_3$:HF:DIW = 0.004:8:50 at room temperature for 10 s. The second step used varying concentrations, temperatures, and reaction times of $AgNO_3$:HF:H_2O_2: DIW, as detailed in Table 1. Ag nanoparticles were removed by immersing the wafers in H_2O_2:$NH_3.H_2O$ (1:3) for 90 s at room temperature. The NSR process was applied using a sodium hydroxide and isopropyl alcohol solution (NaOH:IPA:DIW) for 10 min at 75°C.

TABLE 1. Experimental groups of silicon wafers for studying the effects of parameters in the silver-assisted chemical etching process and subsequent NSR process using a NaOH:IPA:DIW solution. (DIW volume: 25 ml)

Groups	HF:H_2O_2 (ml)	Time (s)	Temperature (°C)
TA1	4:6 6:8 8:10	70	55
TA2	8:10	60 70 80	55
TA3	8:10	60	45 50 55
TA4	6:8 8:10 10:12	60	50

We selected wafers etched with the MACE process under conditions of $HF:H_2O_2 = 4:6$, 70 s, and 55°C to test the sodium silicate solution for the NSR process, as outlined in Table 2.

TABLE 2. Group division of silicon wafers for studying the effects of Na_2SiO_3 concentration and etching time in the NSR process (DIW volume: 25 ml).

Groups	Na_2SiO_3 (g)	IPA (ml)	Temperature (°C)	Time (min)
TA5	1.5	0.5	80	1 2 3
TA6	1.5 2 5	0.5	80	1

After measuring the reflectance and obtaining the NSR conditions that yielded the lowest reflectance (Na_2SiO_3:IPA:DIW = 5:0.5:25, 1 min, 80°C), the NSR process was performed on the etched wafers, as shown in Table 3.

TABLE 3. Group division of silicon wafers for studying the effects of parameters in the two-step silver-assisted chemical etching process, followed by the NSR process using a Na_2SiO_3:IPA:DIW solution.

Groups	$HF:H_2O_2$ (ml)	Time (s)	Temperature (°C)
TA7	6:8 8:10 10:12	60	50
TA8	8:10	60 70 80	50

The reflectance of the wafers was measured using a Shimadzu UV-2550, and the wafers were imaged by field emission scanning electron microscopy (FESEM) (ZEISS SIGMA FE-SEM).

Results and Discussion

In the first step, silver nanoparticles were deposited on silicon wafers using an $AgNO_3$:HF precipitation solution through a galvanic displacement reaction, where two simultaneous processes occur on the silicon surface [12]:

Cathode reaction:

$$2H^+ + 2e^- \longrightarrow H_2 \quad (1)$$

$$Ag^+ + e^- \longrightarrow Ag \quad (2)$$

Anode reaction:

$$Si + 2F^- \longrightarrow SiF_2 + 2e^- \quad (3)$$

$$Si + 2F^- + 2H^+ \longrightarrow SiF_2 \quad (4)$$

After the silver particle deposition process, the silicon wafers were placed in the etching solution ($HF:H_2O_2$). The presence of silver particles on the wafer surfaces stimulates the etching of silicon. Holes are generated through redox reactions at the interface between the metal particles and etching solution. According to Eq. (5), the metal catalyzes the process of reduction of the oxidizing agent (H_2O_2), which subsequently injects holes into the silicon surface directly under the metal particles [29]:

$$H_2O_2 + 2H^+ \longrightarrow 2H_2O + 2h^+ \quad (5)$$

The open space around the metal particles allows the etching solution to penetrate, oxidize the silicon, and dissolve it using HF. Thus, the metal particle penetrates the silicon surface. Immediately below the metallic particle, the hole density is high, as silicon is removed extensively there. The silicon is first oxidized by the process described in Eq. (6), and then the oxide is dissolved by HF, as shown in Eq. (7) [30]:

$$Si + H_2O_2 + 4h^+ \longrightarrow SiO_2 + 4H^+ \quad (6)$$

$$SiO_2 + 6HF \longrightarrow H_2SiF_6 + 2H_2O \quad (7)$$

After etching in the $HF:H_2O_2$ solution, FESEM images showed that the rough surface of black silicon possesses sponge-like nanostructures, with random formation of nonporous, as seen in Fig. 1(a). This structure resulted in a reflectance of 3%, as seen in Fig. 1(b), when the etching solution concentration was 4:6, the temperature was 55°C, and the etching time was 70 seconds.

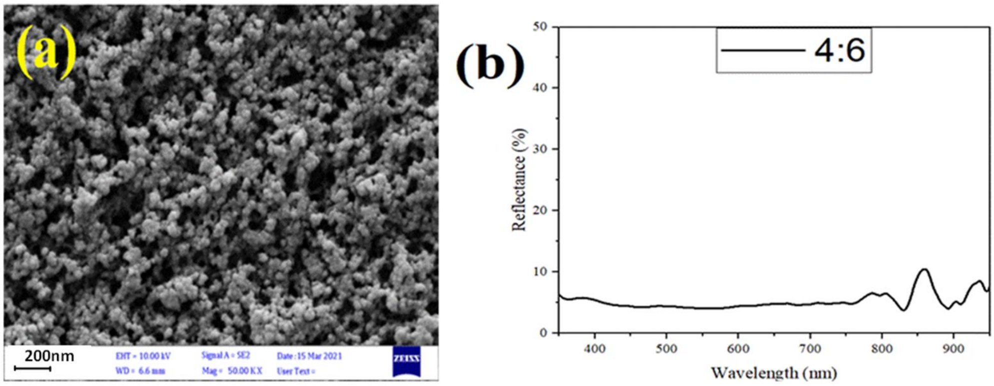

FIG. 1. (a) FESEM image showing the porous structure of the silicon surface. (b) Reflection spectrum as a function of wavelength (350-950 nm) for etched silicon with a concentration of $HF:H_2O_2$=4:6 at 55°C and an etching time of 70 s.

NSR Process by NaOH Solution.

After the etching process, nanostructure rebuilding (NSR) was carried out by immersing the wafers in an alkaline etching solution (NaOH:IPA:DIW). Three groups were prepared to study the effects of the etching solution's material concentration, temperature, and etching time.

Effect of Changing the Concentration of Etching Solution Materials at 55°C for 70 seconds.

In group TA1 (Table 1), we studied the effect of changing $HF:H_2O_2$ ratios while maintaining a fixed DIW volume of 25 ml, with the etching temperature at 55°C and time at 70 s.

The lowest reflection of 12.78% was recorded at a concentration ratio of 8:10 (Fig. 2). The H_2O_2 concentration is crucial for adjusting the silicon nanostructures during the texturization process. Increasing the H_2O_2 concentration raises the silicon etching rate, leading to the formation of nanostructures with porous walls due to the presence of metallic nanoparticles [31]. These porous walls can be etched later by the NSR process, forming new structures on the silicon surface, with their shape depending on the depth of the pore structures formed by the metal-assisted etching process [9]. Depending on the concentration of H_2O_2, the precipitated Ag NPs can decompose into Ag^+ ions and re-deposit elsewhere on the silicon, causing the MACE process to restart at those sites [32].

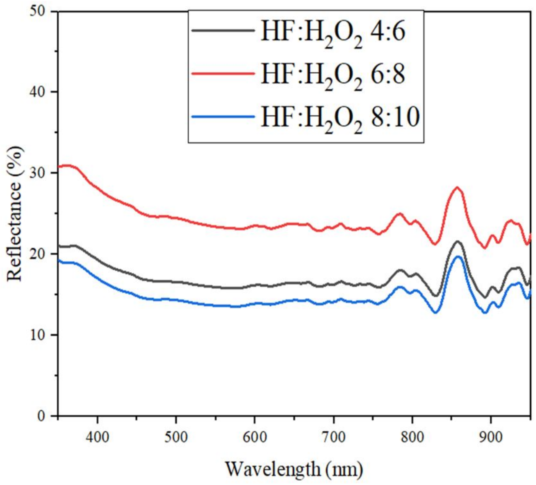

FIG. 2. Reflectance spectra as a function of wavelength (350-950 nm) for silicon wafers of the TA1 group etched with different concentrations of $HF:H_2O_2$.

Fig. 3 shows FESEM images of the silicon after etching with different solution ratios. At a low ratio (4:6), inverted pyramidal structures mixed with deep cavities resulted in a relatively high reflectance of 14.73%, as seen in Fig. 3(a). As the etching solution ratio increased to 6:8, the surface reflectance rose to 20.78%. Figure 3(b) illustrates that the formed cavities had defined walls, with the presence of some inverted pyramid structures separating these deep cavities with flat, empty spaces from any geometric shapes, contributing to the high reflection.

The reflectance decreased to 12.8% with the increase of the ratio of the etching solution to 8:10. The FESEM images in Fig. 3(c) reveal a combination of inverted pyramidal structures and the appearance of moderate pyramidal structures, with deep cavities covering most of the surface.

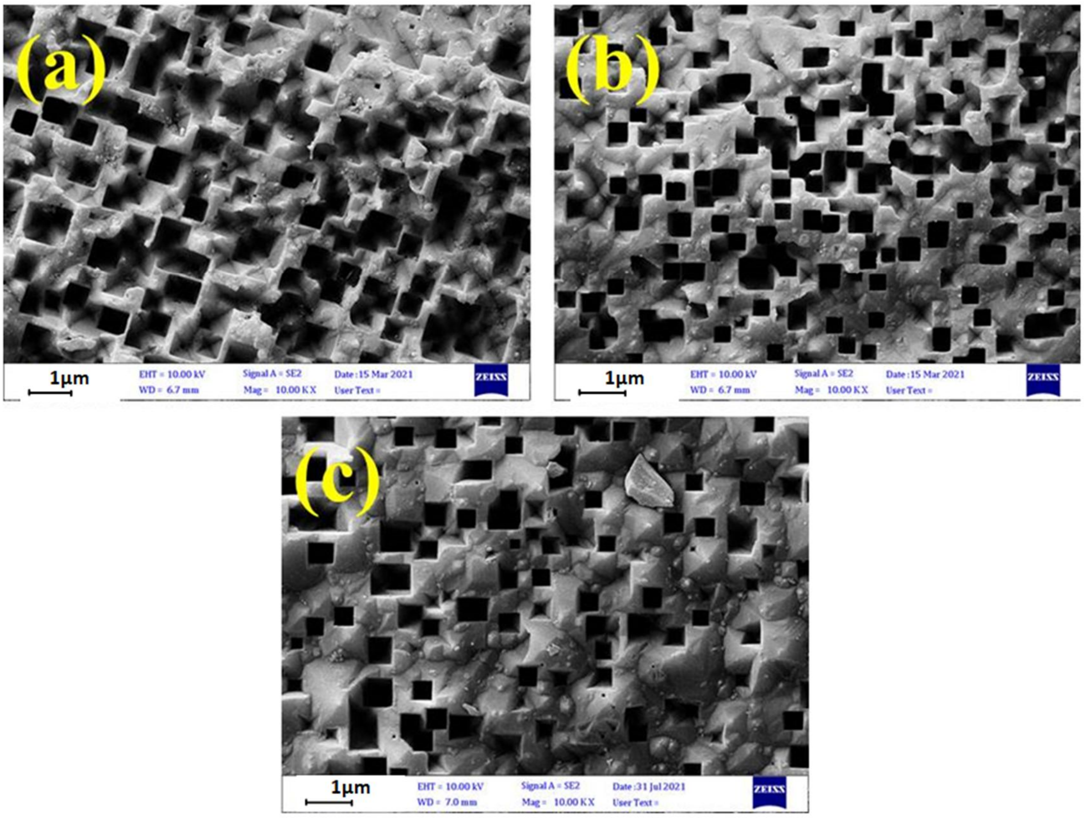

FIG. 3. FESEM images of Si wafers in the TA1 group etched at 55°C for 70 s with different concentrations of HF: H_2O_2: (a) 4:6 ml, (b) 6:8 ml, (c) 8:10 ml.

Effect of Changing the Etching Process Time on the Optical and Morphological Properties of the Wafers.

To study the effect of etching time on silicon reflectance and surface composition, TA2 group samples were prepared with etching times of 60, 70, and 80 s using an 8:10:25 etching solution ratio at 55°C. The lowest reflectance of 11.39% was obtained at 60 s (Fig. 4).

FESEM images in Fig. 5(a) display a defective pyramidal structure overlapping with some deep cavities appearing at an etching time of 60 s. At 70 s, the surface reflectance increased to 12.78%, as the upright pyramid structures disappeared and inverted pyramids appeared alongside deep cavities, as depicted in Fig. 5(b). Further increasing the etching time to 80 s resulted in a higher reflectance of 19.8%, as shown in Fig. 5(c), where deep cavities overlap with flat areas devoid of geometrical structures.

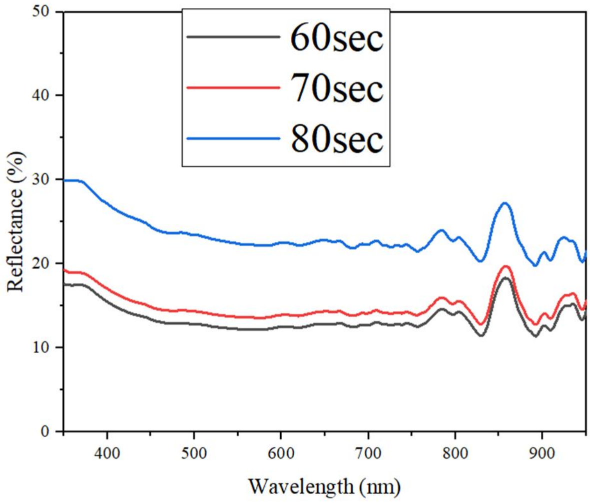

FIG. 4. Reflectance spectra as a function of wavelength (350-950 nm) for TA2 group silicon wafers etched for different durations (60, 70, and 80 s).

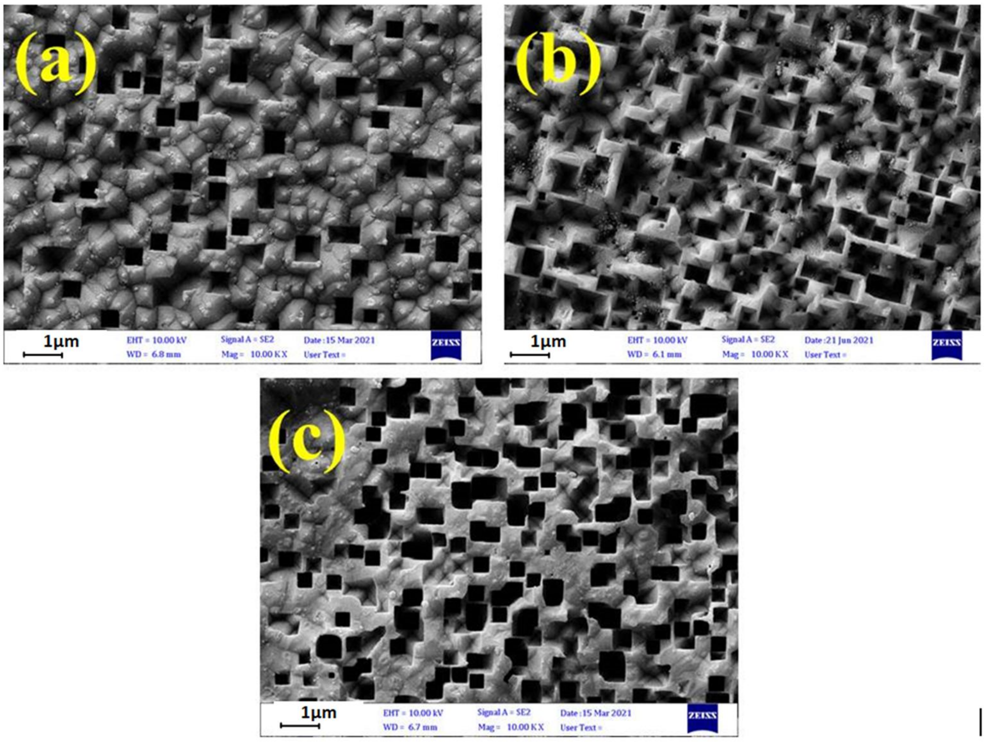

FIG. 5. FESEM images of Si wafers in the TA2 group etched for different durations: (a) 60, (b) 70, and (c) 80 s.

Effect of Changing the Temperature of the Etching Solutions on the Optical and Morphological Properties of the Wafers.

In the TA3 group, we studied the effect of varying the temperature of the etching solution, specifically at 45°C, 50°C, and 55°C. The porous layer formed before the etching process affects the shape and depth of the porous nanostructures formed by the metal-assisted etching process at different temperatures, with the thickness of the black silicon layer increasing at higher temperatures [33].

Fig. 6 shows the reflectance of the wafers. A reflectance of 20.38% was obtained when the temperature of the etching solution was 45°C. This high reflectance can be attributed to the surface morphology, characterized by upright pyramid structures, with some areas still containing silver particles due to the incomplete etching process at a relatively low temperature, as shown in Fig. 7(a).

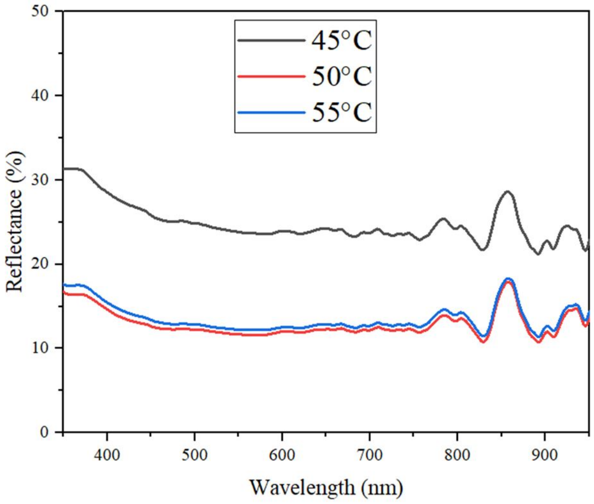

FIG. 6. Reflectance spectra as a function of wavelength (350-950 nm) for TA3 group silicon wafers etched at different temperatures (45°C, 50°C, and 55°C).

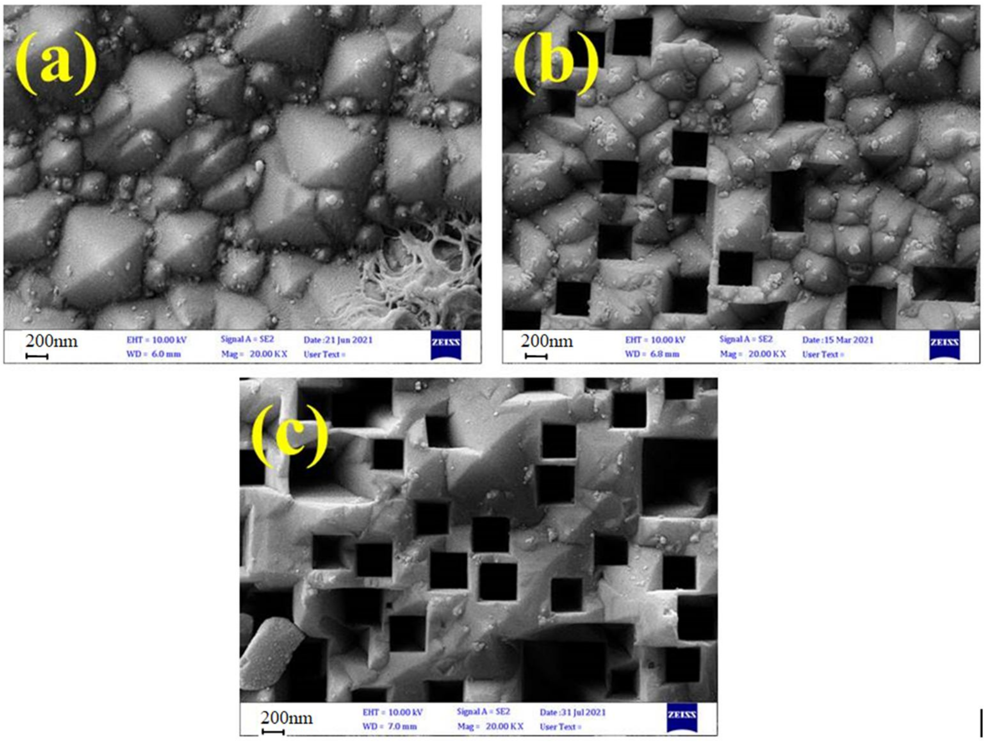

FIG. 7. FESEM image of Si wafers of the TA3 group etched at different temperatures: (a) 45°C, (b) 50°C, and (c) 55°C.

When the temperature was raised to 50°C, the surface reflectance decreased to 10.74% as the silicon surface became covered with moderate hierarchical structures intertwined with deep cavities, as shown in Fig. 7(b). The surface reflectance increased to 11.39% after raising the temperature to 55°C, as the number of deep cavities increased. As for the upright pyramid structures, their number decreased significantly, with flat areas separating the deep cavities, leading to an increase in reflectivity, as seen in Fig. 7(c).

Effect of Changing the Concentration of Etching Solution Materials at a Temperature of 50°C and Etching Time of 60 seconds.

In group TA4, we studied the effect of etching solution material ratios, as outlined in Table 1, with a constant DIW ratio of 25 ml for all solutions, at 50°C and 60 s etching time.

Fig. 8 shows the reflectance spectra of the wafers. A high reflectance of 22.27% was obtained at a low etching solution concentration of 6:8, where the surface structure of the silicon exhibited deep, overlapping cavities, as shown in Fig. 9(a). As the concentration of the etching solution increased to 8:10, the reflectance decreased to 10.74%, and the surface structure transformed into upright pyramidal structures intertwined with deep cavities, as seen in Fig. 9(b). The reflectance rose to 22.51% when the concentration increased to 10:12, and the surface structure changed into irregular pyramids in height, with the inverted pyramidal structures disappearing, as depicted in Fig. 9(c).

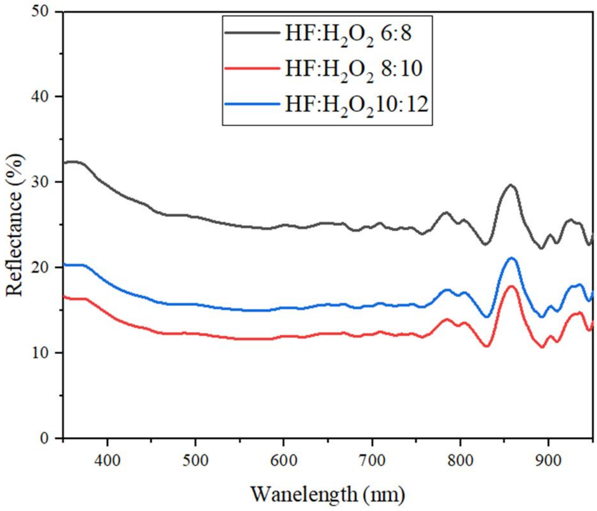

FIG. 8. Reflectance spectra as a function of wavelength (350-950 nm) for silicon wafers in the TA4 group, etched with different concentrations of HF:H_2O_2.

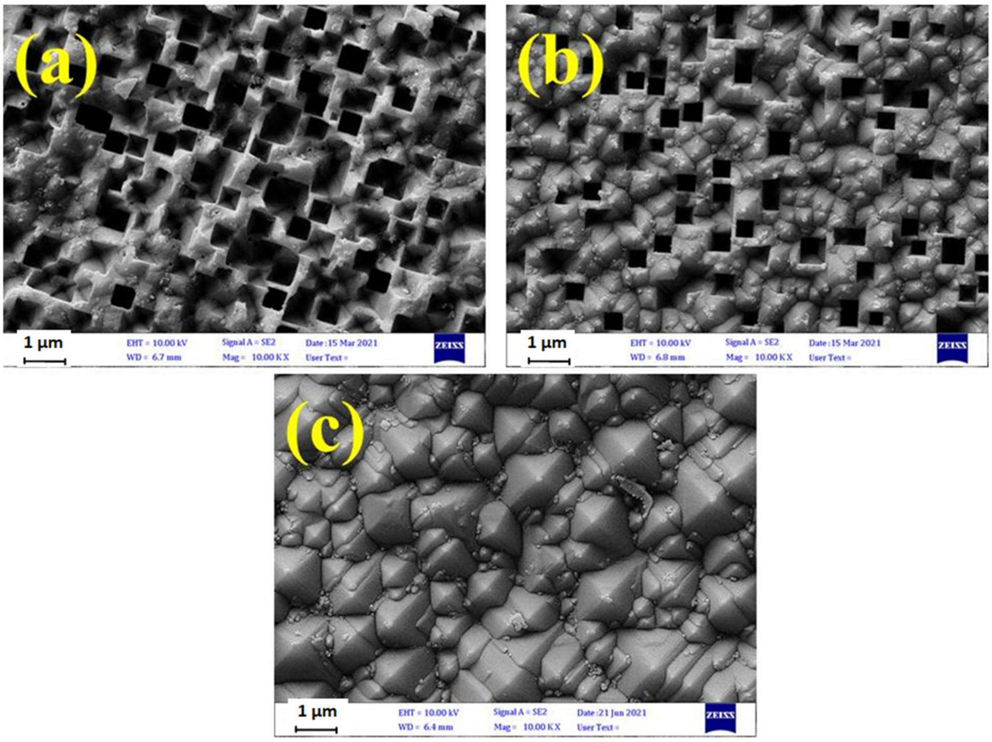

FIG. 9. FESEM images of Si wafers from the TA4 group etched at 50°C for 60 s using different concentrations of HF:H_2O_2: (a) 6:8 ml, (b) 8:10 ml, (c) 10:12 ml.

Texturing Process Using Two-step Ag-assisted Chemical Etching Followed by the NSR Process with Sodium Silicate (Na_2SiO_3) Solution.

The NSR process was performed on wafers that had been etched using a two-step silver-assisted etching method. For the second step of the etching, the conditions were as follows: the etching solution consisted of 4 ml of HF and 6 ml of H_2O_2 added to 25 ml of DIW. The process was conducted at a temperature of 55°C with an etching time of 70 s.

Studying the Effect of Changing the NSR Process Time on the Optical and Morphological Properties of the Wafers.

In group TA5 (Table 2) we studied the effect of NSR etching time while maintaining a constant Na_2SiO_3 concentration (1.5 g) and IPA concentration (0.5 ml) in 25 ml of DIW at a temperature of 80°C. At an etching time of 1 min, a reflectance of 16.68% was obtained, as shown in Fig. 10. FESEM images in Fig. 11(a) revealed a rough surface with deep cavities, free of pyramid structures, resembling a porous surface where the layer was not fully removed.

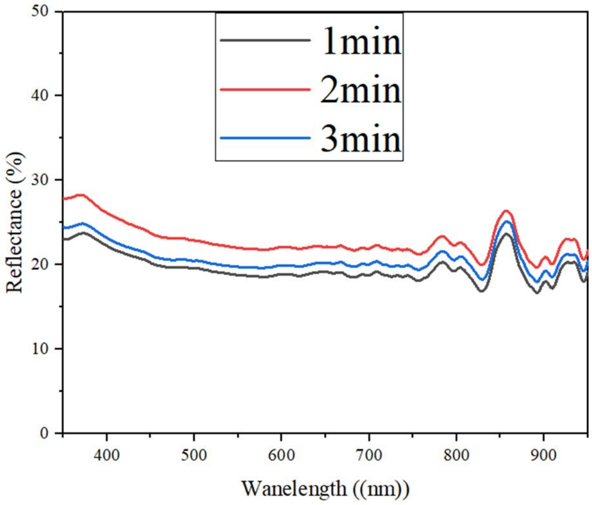

FIG. 10. Reflectance spectra as a function of wavelength (350-950 nm) for silicon wafers group TA5, processed with the NSR method at different etching times (1, 2, and 3 min).

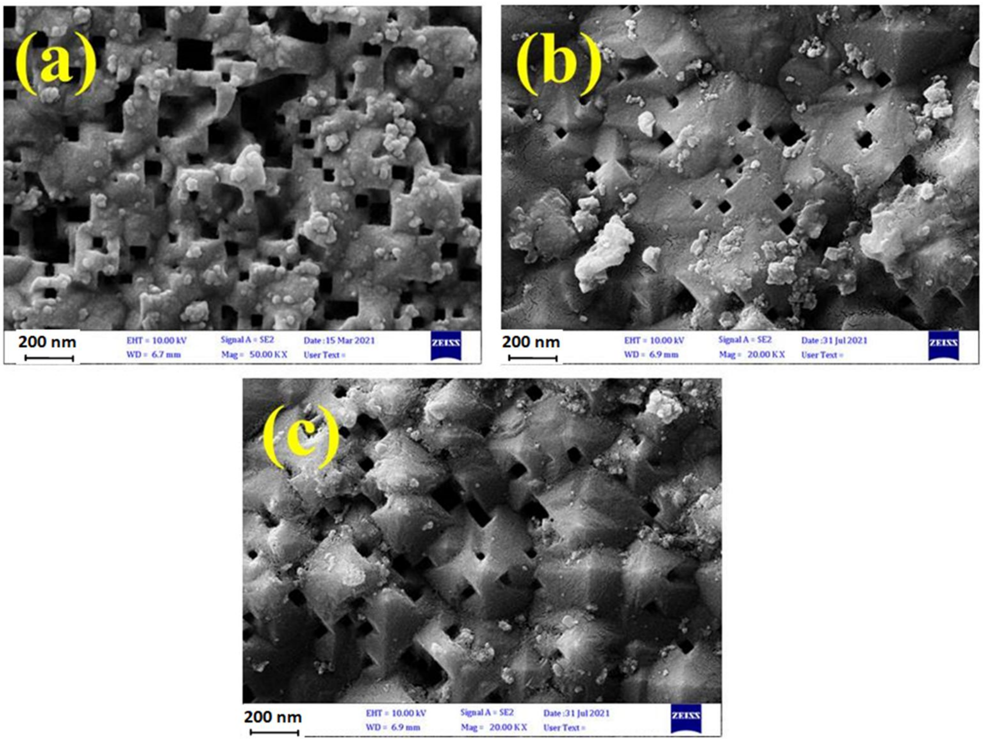

FIG. 11. FESEM image of Si wafers in group TA5 etched using the NSR process at different etching times: (a) 1 min, (b) 2 min, and (c) 3 min.

As the etching time increased to 2 min, surface reflection rose to 19.68%. The FESEM images in Fig. 11(b) show that the surface became irregular and free of pyramid structures, with small pores present. At an etching time of 3 min, the reflection decreased to 17.89% as the etching depth increased, causing the porous layer to disappear and pyramid structures to appear, interspersed with deep cavities, as seen in Fig. 11(c).

Study of the Effect of Changing the Na_2SiO_3 Concentration in the NSR Process on the Optical and Morphological Properties of Wafers.

In group TA6 (Table 2), we investigated the effect of changing the concentration of Na_2SiO_3 in the etching solution (1.5, 2 and 5 g), while keeping the IPA concentration fixed at 0.5 ml, the etching time at 1 min, and the temperature at 80°C. At a low Na_2SiO_3 concentration of 1.5 g, a reflectance of 16.68% was obtained (Fig. 12). The silicon surface exhibited a rough texture with deep intervening cavities, similar to a porous surface and free of pyramid structures, as seen in Fig. 13(a).

With the increase of the concentration to 2 g, the surface reflectance decreased to 14.23%, and a rough surface was formed as seen in Fig. 13(b), with the disappearance of overlapping deep pores. At a concentration of 5 g, the reflectance decreased to 8.65%, with the formation of a rough surface characterized by non-overlapping pores with a smaller cross-section, as shown in Fig. 13(c).

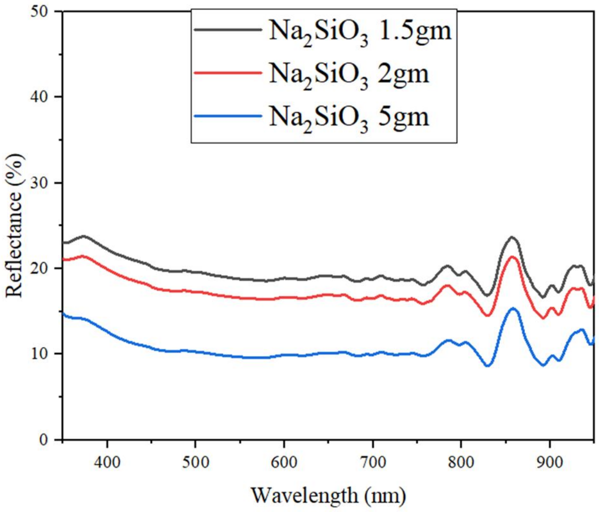

FIG. 12. Reflectance spectra as a function of wavelength (350-950 nm) for silicon wafers in group TA6, processed with the NSR method at different Na_2SiO_3 concentrations (1.5, 2, and 5 g).

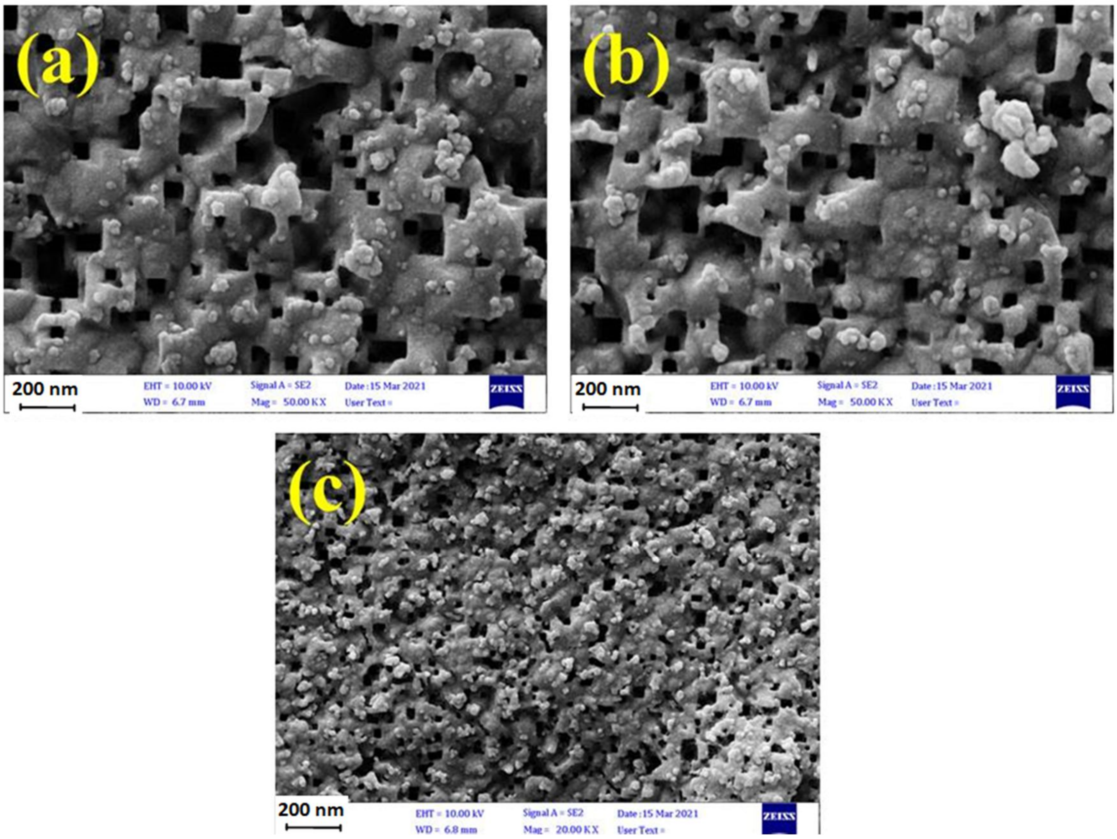

FIG. 13. FESEM images of Si wafers in group TA6 etched with different concentrations of Na_2SiO_3: (a)1 g, (b) 2 g, and (c) 5 g.

Testing the Effect of the NSR Process on the Optical Properties of Etched Wafers Using Different Etching Solution Concentrations and Etching Times.

We also tested the NSR process on wafers textured by a two-step silver-assisted etching process at different etching times and concentrations while maintaining a constant temperature of 50°C. For the NSR process, the etching solution concentration was Na_2SiO_3:IPA:DIW = 5:0.5:25, with an etching time of 1 min at a temperature of 80°C.

Effect of Changing the Etching Solution Concentration on the Optical Properties of the Wafers.

In group TA7, we studied the effect of the concentration of etching solution materials ($HF:H_2O_2$:DIW) in different ratios (6:8, 8:10, and 10:12) at a temperature of 50°C and an etching time of 60 s. The reflectance measurements for the TA7 wafers are shown in Fig. 14. The results were very similar across the different concentrations, with the lowest reflectance of 24.88% obtained at a concentration of (6:8).

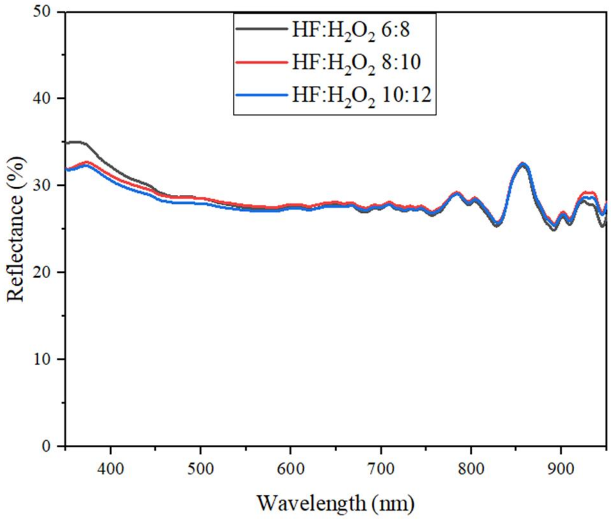

FIG. 14. Reflectance spectra as a function of wavelength (350-950 nm) for silicon wafers of the TA7 group etched at different etching solution concentrations (6:8, 8:10, and 10:12).

The Effect of Changing the Etching Process Time on the Optical Properties of the Wafers

In the TA8 group, the effect of the etching process time (60, 70, and 80 s) was tested at a temperature of 50°C with an etching solution concentration of 8:10. The wafer reflection is shown in Fig. 15. The reflectance measurements were similar across the samples, with the lowest reflectance of 18.34% observed an etching time of 80 s.

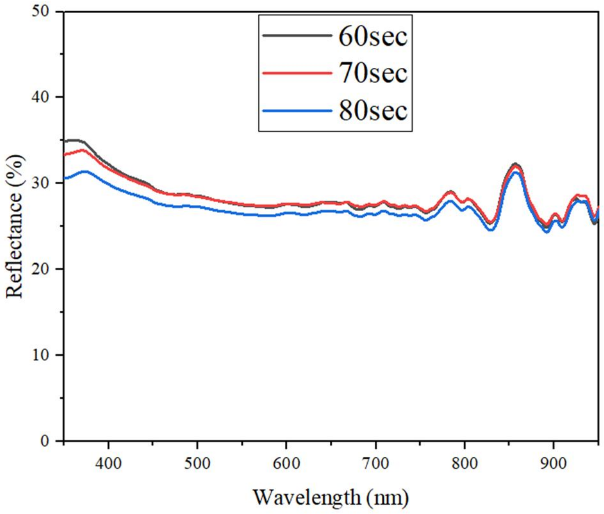

FIG. 15. Reflection spectra as a function of wavelength (350-950 nm) for silicon wafers in the TA8 group at different etching times (60, 70, and 80 s).

Conclusion

In our work, we investigated the effect of the NSR process on the wafers that were textured using a two-step silver-assisted chemical etching process. The NSR process was performed on the wafers after the metal-assistance etching process to change the shape of the surface structure from black porous silicon to pyramid structures, deep pores, and a rough surface with small pores.

For the NSR process, two solutions were tested. The first solution consisted of sodium hydroxide and isopropyl alcohol. We examined the effects of the etching process parameters, including materials concentration, etching time, and temperature. When studying the concentration of the etching solution, the lowest reflection of 12.78% was obtained with an NSR process ratio of $HF:H_2O_2 = 8:10$. In terms of etching time, the minimum reflection of 11.39% was obtained with an etching duration of 60 seconds. Regarding temperature, the lowest reflection of 10.74% occurred at 50°C, resulting in surface structures that featured pyramids overlapping with deep cavities.

When using sodium silicate (Na_2SiO_3) solution and isopropyl alcohol (IPA) in the NSR process, the effect of the etching process parameters (materials concentration, etching time) was studied. The lowest reflection of 17.89% was observed when the NSR process was performed for 1 minute. Additionally, when the etching solution concentration was Na_2SiO_3:IPA = 5:0.5, the lowest reflection of 8.65% was achieved, and the wafer surfaces exhibited a rough texture.

References

[1] Lai, J,-H., “Development of Low-Cost High-Efficiency Commerical-Ready Advanced Silicon Solar Cells”, (2014).

[2] van Sark, W.G.J.H.M., Alsema, E.A., Junginger, H.M., de Moor, H.H.C., and Schaeffer, G.J., Prog. Photovolt.: Res. Appl., 16 (2008) 441.

[3] IEA-PVPS, Survey Report of Selected IEA Countries between 1992 and 2013, (2014).

[4] Solanki, C.S. and Singh, H.K., “Anti-reflection and Light Trapping in c-Si Solar Cells”, (Singapore: Springer Nature, 2017).

[5] Liu, Y., Zi, W., Liu, S., and Yan, B., Sol. Energy Mater. Sol. Cells, 140 (2015) 180.

[6] Goetzberger, A., Knobloch, J., and Vob, B., “Crystalline Silicon Solar Cells”, (Freiburg, Germany: John Wiley Sons, 1994).

[7] Abushaara, K., Shabat, M., El-Amassi, D., and Schaadt, D., Jordan J. Phys., 13 (1) (2020) 87.

[8] Raval, M.C. and Reddy, S.M., “Industrial Silicon Solar Cells”, In: “Solar Cells”, (Intech Open, 2019).

[9] Lin, Y.K., Chen, Y.S., and Hsueh, C.H., Results Phys., 12 (2019) 244.

[10] Li, S., Ma, W., Zhou, Y., Chen, X., Xiao, Y., Ma, M., Zhu, W., and Wei, F, Nanoscale Res. Lett., 9 (2014) 1.

[11] Rokhinson, L.P., Guo, L.J., Chou, S.Y., and Tsui, D.C., Appl. Phys. Lett., 76(2000) 1591.

[12] Peng, K., Hu, J., Yan, Y., Wu, Y., Fang, H., Xu, Y., Lee, S., and Zhu, J., Adv. Funct. Mater., 16 (2006) 387.

[13] Zhao, J., Wang, A., and Campbell, P., IEEE Trans. Electron. Devices, 46 (1999) 1978.

[14] Willeke, G., Nussbaumer, H.H.B., and Bucher, E., Sol. Energy Mater. Sol. Cells, 26 (1992) 345.

[15] Yuwen, Z., Zhongming, L., Chundong, M, and Shaoqi, H., Sol. Energy Mater. Sol. Cells, 48 (1997) 167.

[16] Inomata, Y., Fukui, K., and Shirasawa, K., Sol. Energy Mater. Sol. Cells, 48 (1997) 237.

[17] Dobrzański, L.A., J. Achiev. Mater. Manuf. Eng., 31 (2008) 77.

[18] Watanabe, R., Abe, S., Haruyama, S., Suzuki, T., Onuma, M., and Saito, Y., Int. J. Photoenergy, 2013 (2013) 1.

[19] Zubel, I., Rola, K., and Kramkowska, M., Sensors Actuators, A Phys., 171 (2011) 436.

[20] Wang, Y., Yang, L., Liu, Y., Mei, Z., Chen, W., Li, J., Liang, H., Kuznetsov, A., and Xiaolong, D., Sci. Rep., 5 (2015) 1.

[21] Yang, W., Shen, H., Jiang, Y., Tang, Q., Raza, A., and Gao, K., Phys. Status Solidi Appl. Mater. Sci., 216 (2019) 1.

[22] Zhong, S., Wang, W., Zhuang, Y., Huang, Z., and Shen, W., Adv. Funct. Mater., 26 (2016) 4768.

[23] Fang, H., Wu, Y., Zhao, J., and Zhu, J., Nanotechnology, 17 (2006) 3768.

[24] Li, X. and Bohn, P.W., Appl. Phys. Lett., 77 (2000) 2572.

[25] Tsujino, K. and Matsumura, M., Adv. Mater., 17 (2005) 1045.

[26] Tang, Q., Shen, H., Yao, H., Jiang, Y., Li, Y., Zhang, L., Ni, Z., and Wei, Q., Appl. Surf. Sci., 455 (2018) 283.

[27] Pu, T., Shen, H., Zheng, C., Xu, Y., Jiang, Y., Tang, Q., Yang, W., Rui, C., and Li, Y., Energies, 13 (2020) 4890.

[28] Chen, K., Zha, J., Hu, F., Ye, X., Zou, S., Vähänissi, V., Pearce, J.M., Savin, H., Su, X., and Pearce, J.M., Sol. Energy Mater. Sol. Cells, 191 (2019) 1.

[29] Chartier, C. and Bastide, S., Electrochim. Acta, 53 (2008) 5509.

[30] Xia, X.H., Ashruf, C.M.A., French, P.J., and Kelly, J.J., Chem. Mater, 12 (2000) 1671.

[31] Qu, Y., Liao, L., Li, Y., Zhang, H., Huang, Y., and Duan, X., Nano Lett., 9 (2009) 4539.

[32] Zhong, X., Qu, Y., Lin, Y.-C., Liao, L., and Duan, X., Acs. Appl. Mater. Interfaces, 3 (2011) 261.

[33] Tang, Q., Shen, H., Yao, H., Gao, K., Jiang, Y., Yang, W., and Liu, Y., Sol. Energy, 170 (2018) 263.